Investigating Buried Ice at Askja Volcano, Northern Iceland using Ground Penetrating Radar: A Planetary Analog Perspective

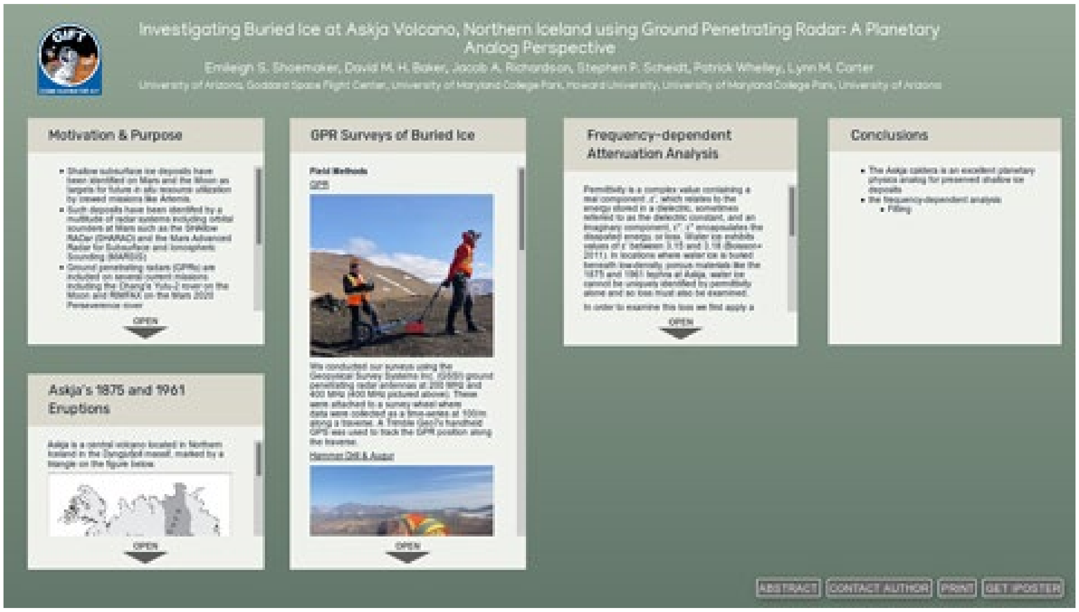

Emileigh S. Shoemaker, David M. H. Baker, Jacob A. Richardson, Stephen P. Scheidt, Patrick Whelley, Lynn M. Carter

University of Arizona, Goddard Space Flight Center, University of Maryland College Park, Howard University, University of Maryland College Park, University of Arizona

PRESENTED AT:

AGU FALL MEETING
Online Everywhere | 1–17 December 2020

MOTIVATION & PURPOSE

- Shallow subsurface ice deposits have been identified on Mars and the Moon as targets for future *in situ* resource utilization (ISRU) by crewed missions like Artemis.
- Such deposits have been identifed by a multitude of radar systems including low-frequency orbital sounders at Mars such as the SHAllow RADar (SHARAD) and the Mars Advanced Radar for Subsurface and Ionospheric Sounding (MARSIS)
- Ground penetrating radars (GPRs) are included on several current missions including the Chang'e Yutu-2 rover on the Moon and RIMFAX on the Mars 2020 Perseverence rover
- GPR is well-suited to detect reservoirs of preserved water ice in the subsurface and could be used as a prospecting tool by crewed missions in order to find it
- **Key Question: How can we uniquely identify water ice using GPR that has been preserved beneath low-loss, porous media such as volcanic ash, tephra, or sediment?**

ASKJA'S 1875 AND 1961 ERUPTIONS

Askja is a central volcano located in Northern Iceland in the Dyngjufjoll massif, marked by a triangle on the figure below.

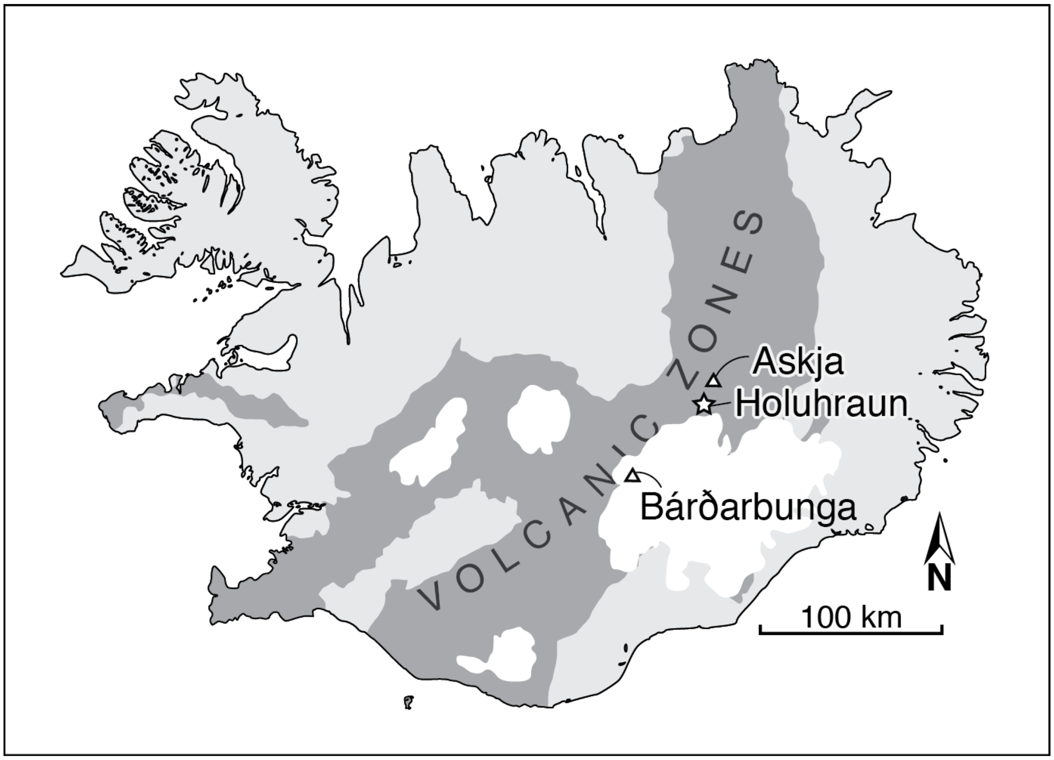

We investigated a region of interest (blue box) where two eruptions of Askja potentially preserserving ice overlap within the caldera.

1875 Eruption

- Major phreatoplinian eruption in March 1975 (Sparks+ 1981, Carey+ 2009)
- Formed ~11 km^2 Lake Oskjuvatn and later the small geothermal lake Viti
- Erupted a buff-colored, subangular, rhyolitic pumice across almost 7500 km^2 of eastern Iceland (Sparks+ 1981) and 3 km^3 of ash atop seasonal snowfall

1961 Eruption

- Effusive, basaltic eruption in October 1961 (Thorarinsson & Sigvaldason, 1962)
- Emplaced ~11 km^2 of basaltic lava eastward from the rim of the caldera
- Erupted a brown-black tephra atop seasonal snowfall

GPR SURVEYS OF BURIED ICE

Field Methods

GPR

We conducted our surveys using the Geopysical Survey Systems Inc. (GSSI) ground penetrating radar antennas at 200 MHz and 400 MHz (400 MHz pictured above). These were attached to a survey wheel where data were collected as a time-series at 100/m along a traverse. A Trimble Geo7x handheld GPS was used to track the GPR position along the traverse.

Hammer Drill & Augur

A hammer drill with an augur was used to retrieve core samples down to 1.5 m at locations where buried ice may have been detected by the GPR.

UAV

Aerial images were taken of the survey sites within the caldera with a DJI Mavic 2 Pro quadcopter. These were used to produce an orthomosaic and digital terrain model (DTM) of the region of the caldera where the surveys were conducted.

Identifying Buried Water Ice Using GPR

1. Identify reflectors - horizons in the subsurface produced by significant density contrasts as the radar wave travels through layers of different media
2. Calculate the permittivity - tied closely to the composition of the media in the subsurface

3. Look at the losses of the radar wave as it travels at different frequencies - are differences in loss visible between unconsolidated tephra and ice?

Results

We conducted 51 GPR surveys in the caldera at both frequencies. Additionally we drilled 11 boreholes and 3 trenches in order to confirm the presence of ice and other stratigraphy at several sites of interest.

A meltwater-derived channel with ice preserved by tephra from both the 1875 and 1961 eruptions will be the focus of several interesting results from these surveys (shown below). White lines indicate locations of GPR traverses on either bank of the meltwater channel at both 200 MHz and 400 MHz.

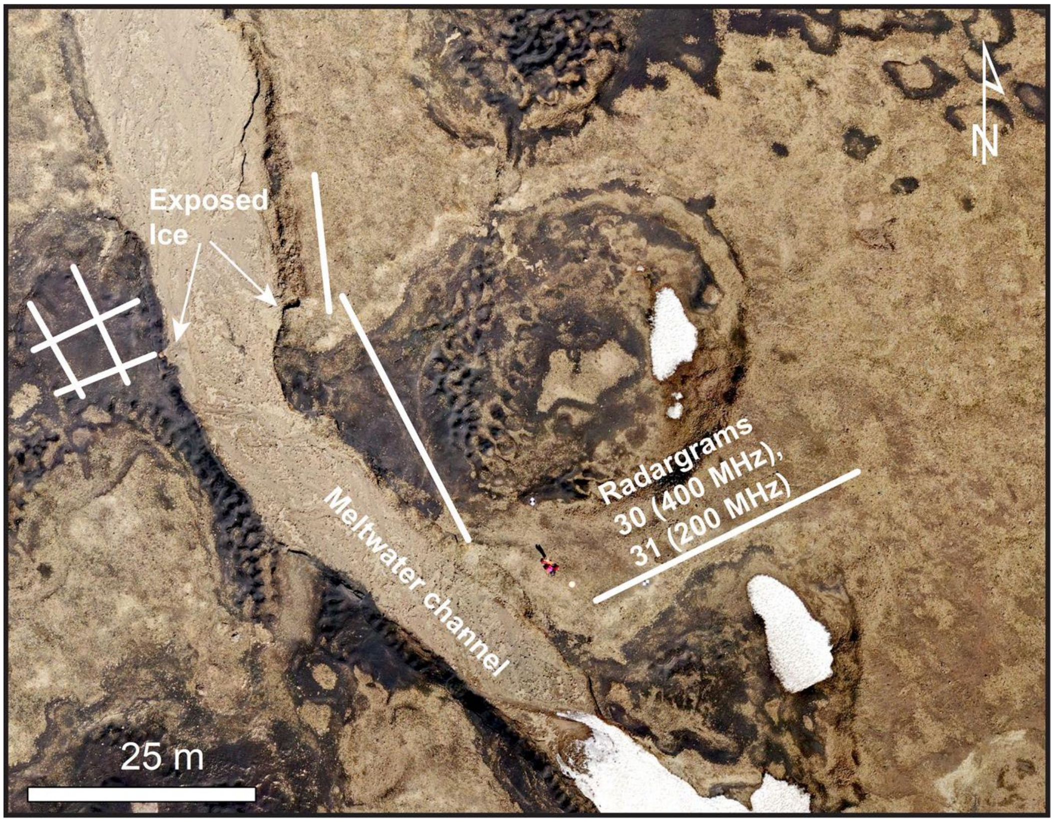

Sites where ice was uncovered along the banks are included below.

An example of how the data are collected along a traverse at this site can be viewed in the linked video below.

[VIDEO] https://www.youtube.com/embed/BmBdNO2MLKw?rel=0&fs=1&modestbranding=1&rel=0&showinfo=0

More than 2 m of massive ice has been uncovered preserved beneath the 1875 pumice (pictured below).

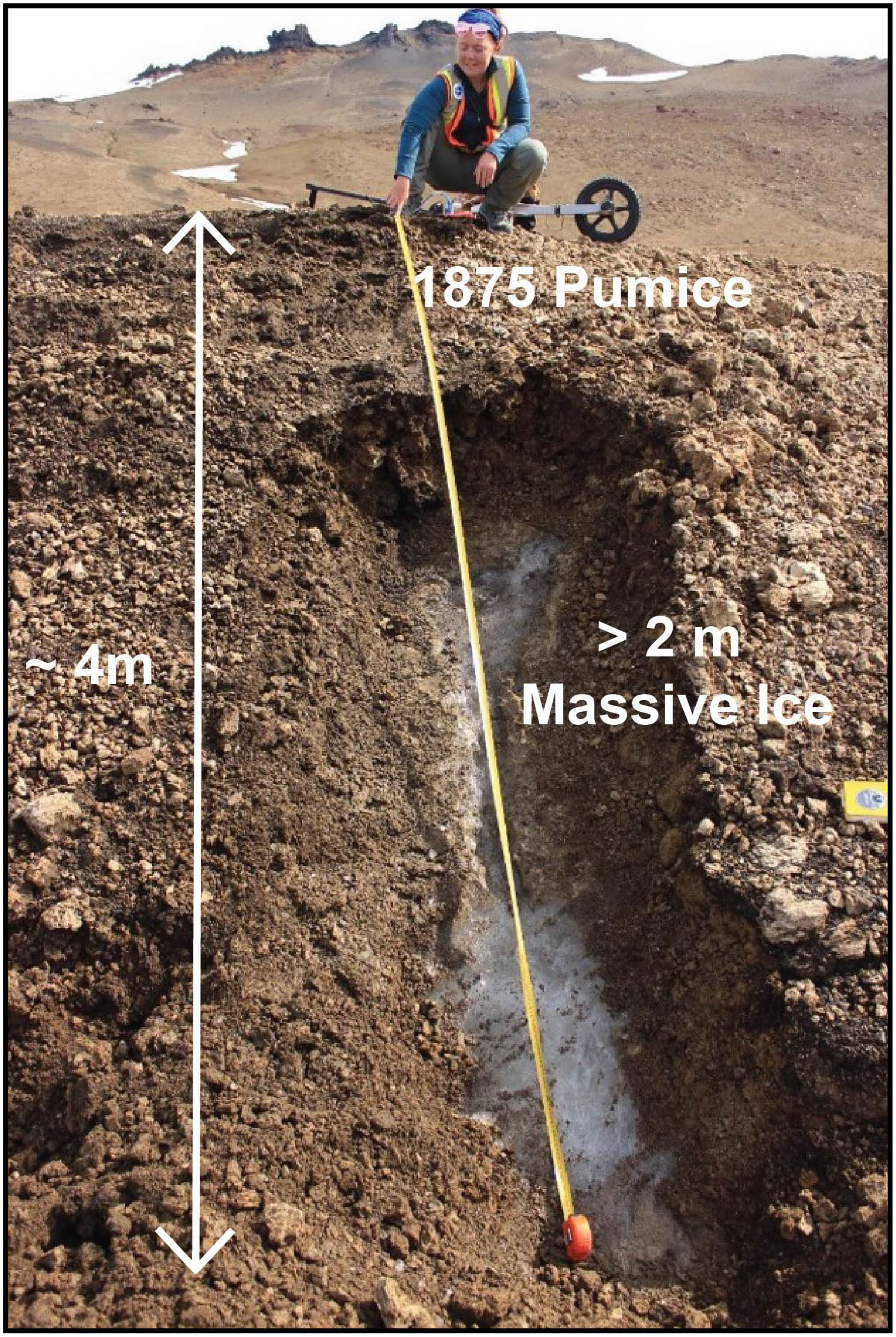

≥ 60 cm of ice has been found beneath the 1961 tephra deposit (pictured below) and deposited on top of 1875 materials.

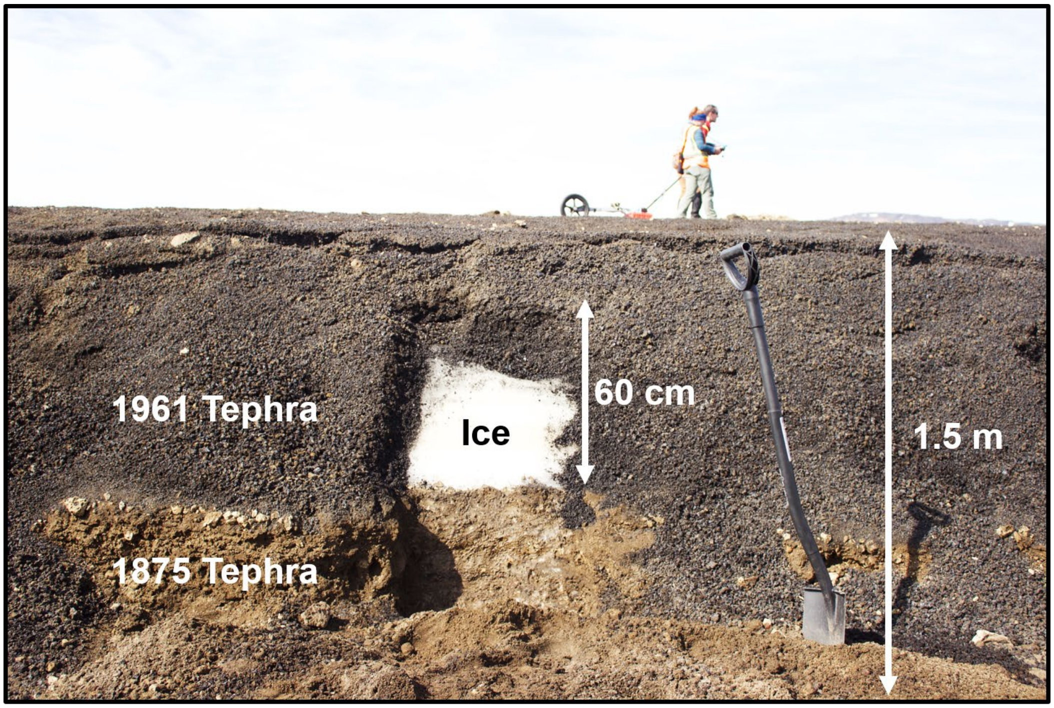

Traverses with the GPR at both 200 and 400 MHz antennas were taken at both of these locations.

Radargrams produced near this location will be shown in the image slider to the right. We will examine the frequency-dependent attenuation of the radar signal at 200 and 400 MHz. Radargrams 30 (400 MHz) and 31 (200 MHz) will be analyzed and discussed in the next panel.

$$\frac{P_R}{P_T} = \frac{G^2\lambda^2\xi}{64\pi^3R^4}e^{-4\alpha R}$$

R T

$$\alpha = \frac{\omega}{c}\sqrt{\frac{\varepsilon'}{2}\left(\sqrt{1+\left(\frac{\varepsilon''}{\varepsilon'}\right)^2}-1\right)}$$

FREQUENCY-DEPENDENT ATTENUATION ANALYSIS

Permittivity is a complex value containing a real component ,ε', which relates to the energy stored in a dielectric, sometimes referred to as the dielectric constant, and an imaginary component, ε''. ε'' encapsulates the disspated energy, or loss. Water ice exhibits values of ε' between 3.15 and 3.18 (Boisson+ 2011). In locations where water ice is buried beneath low-density, porous materials like the 1875 and 1961 tephra at Askja, water ice cannot be uniquely identified by permittivity alone and so loss must also be examined.

In order to examine this loss we remove all applied gains and apply a background removal filter to remove coherent noise. We then average traces of interest where the reflector at the contact of the ice base and material below is consistent and not changing depth. This produces a single averaged trace of power with depth.

The peaks of this average trace are selected using local maxima and then can be fit with a curve describing the two-way total attenuation per meter depth associated with the transmission of the radar wave through the media in the subsurface.

Here we model geometric spreading and dielectric losses after the methods detailed in Boisson+ (2011). We consider three such models assuming different backscattered cross sections.

Geometric spreading is the result of the increased area of the wavefront as it propagates and can be described by radar equation (Stratton, 1941; Skolnik, 1990)

$$\frac{P_R}{P_T} = \frac{G^2\lambda^2\xi}{64\pi^3R^4}e^{-4\alpha R}$$

where P_R and P_T are the received and transmitted powers, respectively, G is the antenna gain, λ is is the radar wavelength in the medium, R is the distance from the antenna to the target, and ξ is the backscattered cross section for which we consider three models from Boisson+ (2011).

α is the dielectric loss, in decibels per meter, and is the result of a decrease of electric field amplitude as the wave propagates into an attenuating dielectric and is given by

$$\alpha = \frac{\omega}{c}\sqrt{\frac{\varepsilon'}{2}\left(\sqrt{1+\left(\frac{\varepsilon''}{\varepsilon'}\right)^2}-1\right)}$$

where ω is the angular frequency of the radar, c is the speed of light, and the ratio of ε'' and ε' is the loss tangent tanδ.

To describe the backscattered cross sections we consider three models as in Boisson+ (2011): an infinite, smooth planar reflector where P_R/P_T is effectively $1/R^2$, a rough planar reflector in which the radar echoes are integrated over the first Fresnel zone where P_R/P_T is effectively $1/R^3$, and Rayleigh scatterers which are spheres at subwavelength scales where P_R/P_T is effectively $1/R^4$.

Plots of these models and the total loss are shown in the image slider to the right for 0-14 m along radargrams 30 (400 MHz) and 31 (200 MHz).

If these losses are subtracted from the total loss, the residual losses can be attributed to scattering of the radar wave from localized interfaces within the subsurface and can be a large contributer when the scale of the embedded objects approaches the wavelength of the radar.

ABSTRACT

Shallow subsurface ice deposits on Mars and the Moon have been identified as potential targets for *in situ* resource utilization by future crewed missions to the surfaces of these bodies. On Mars, such deposits have been identified through a variety of orbital measurements at the poles, mid-latitudes, and even preserved by volcanic ash near the Tharsis Montes. At some locations, massive ice deposits have been documented to be 100 m in thickness at depths as shallow as 1 m. On the Moon, the presence of thick, massive ice has not been confirmed; however, orbital observations indicate that the upper 1-2 m of regolith may contain a few weight percent in thermally favorable locations. Eruptions of the Askja Volcano in March, 1875 and November, 1961 deposited abundant pyroclasts, which blanketed and insulated fresh snowfall that later densified into massive ice and is preserved today. The pyroclasts consist of a buff colored pumice from the eruption in 1875 and basaltic lapilli and ash from the eruption in 1961. The largely unvegetated, unconsolidated nature of the pyroclasts and their stratigraphic relationships with shallow subsurface ice make them potentially analogous to some ice deposits within regolith and pyroclasts at the Moon and Mars. Ground penetrating radar (GPR) can be used by future human or robotic missions to identify water ice similarly preserved in the shallow subsurface of these bodies. Our team conducted over 66 GPR surveys inside and surrounding the Askja caldera in August 2019 at 200 and 400 MHz to map both the volcanic deposits and the subsurface ice deposits. We also used a hammer drill augur to take boreholes in order to confirm subsurface stratigraphy and the presence of ice down to 1-1.5 m and aerial surveys using a Mavic 2 Pro quadcopter at each site for additional context. We observed shallow ice deposits within pore spaces of the pyroclasts at depths of ~15-30 cm and pure ice deposits at varying depths (0.6-1 m) as thick as 2-3 m. We also plan to use the data to characterize the frequency-dependent attenuation of the radar signal as it travels through volcanoclastic material and ice in the subsurface. Our investigation of Askja as a planetary analog will provide insight into analytical methods that can be used to investigate subsurface water ice from surface operations at other terrestrial bodies.